

Random disorder and the smectic-nematic transition in liquid-crystalline elastomersWim H. de Jeu,^{1,*} Boris I. Ostrovskii,² Dominic Kramer,³ and Heino Finkelmann³¹*Polymer Science and Engineering, University of Massachusetts, Amherst, Massachusetts 01003, USA*²*Institute of Crystallography, Academy of Sciences of Russia, Leninsky prospect 59, 117333 Moscow, Russia*³*Institut für Makromolekulare Chemie, Albert-Ludwigs-Universität Freiburg, D-79104 Freiburg, Germany*

(Received 28 August 2010; revised manuscript received 25 November 2010; published 6 April 2011)

We report effects of disorder due to random cross-linking on the nematic to smectic-A phase transition in smectic elastomers. Thermoelastic data, stress-strain relations and high-resolution x-ray scattering profiles have been analyzed for two related compounds with a small and a larger nematic range, respectively, each for 5% as well as 10% cross-links. At 5% cross-link density the algebraic decay of the positional correlations of the smectic layers survives in finite-size domains, providing a sharp smectic-nematic transition. At an increased cross-link concentration of 10% the smectic order disappears and gives way to extended short-range layer correlations. In this situation neither a smectic-nematic nor a nematic-isotropic transition is observed anymore. The occurrence of disorder at a relatively large cross-link concentration only, indicates that smectic elastomers are rather resistant to a random field. The temperature dependence of the correlation lengths and thermoelastic behavior suggest a shift to a “parasmectic” regime of a first-order smectic-isotropic transition.

DOI: [10.1103/PhysRevE.83.041703](https://doi.org/10.1103/PhysRevE.83.041703)

PACS number(s): 61.30.Eb, 61.05.cf, 61.41.+e, 64.60.Cn

I. INTRODUCTION

Phase transitions in liquid crystals have attracted interest because they show a wealth of symmetry-breaking scenarios and enable tests of the modern theories of critical phenomena [1]. In this context, smectic liquid-crystal (LC) systems are of particular interest. They consist of stacks of liquid layers in which the rodlike molecules possess orientational order of their long molecular axes, defining the director $\mathbf{n}(\mathbf{r})$. The order of the smectic layers is characterized by a two-component order parameter $\psi(\mathbf{r})$ in three-dimensional (3D) space. Due to its 1D character, the smectic periodicity is unstable to long-wavelength thermal layer fluctuations (Landau-Peierls instability) [2,3]. As a result, the positional correlations decay algebraically as $r^{-\eta}$, η being small and positive, and the discrete Bragg peaks change into singular diffuse scattering with an asymptotic power-law form [4]. This type of anisotropic line shape was first observed in low-molecular-mass thermotropic smectic phases by Als-Nielsen *et al.* [5] and subsequently also for lyotropic lamellar phases [6–8], smectic polymers [9], and lamellar block copolymers [10]. Upon heating, the smectic layers may melt into a nematic phase in which only orientational order survives. An interesting new element has been introduced by subjecting the corresponding smectic-A nematic (SmA-*N*) phase transition to an external random field. As is well documented, the effects of random disorder on phase transitions can be dramatic, leading to the destruction of long-range order, smearing of phase transitions, production of new exotic phases, etc. Examples in crystals comprise the pinning of an Abrikosov flux vortex lattice by impurities in superconductors [11] and random-field Ising magnets [12]. Regarding the first example, Larkin [13,14] predicted that at large enough length scales, even a weak random field should destroy translational order, resulting in exponentially decaying positional correlations. Later work [15] recognized

that the effect of the disorder was overestimated and that quasi-long-range order can survive (positional correlations decaying algebraically at large distances). The latter property is similar to the behavior of solids in 2D as well as layer correlations in a smectic LC [1]. In liquids, disorder has been introduced by confining superfluid helium to a random porous medium [16]. Similarly, monomeric liquid crystals showing a SmA-*N* phase transition have been confined to the connected void space of an aerogel (aerosil). These consist of a highly porous fractal-like network of multiply connected filaments of aggregated silica spheres that form a random network providing pinning of the smectic layers. As a result, even at low density of the aerogels or aerosils (about 1%–3%), the smectic order is destroyed and persists only locally [17–22]. This behavior is in agreement with theoretical predictions that generic quenched disorder should do so, no matter how weak [23,24]. In the present paper, we investigate the SmA-*N* phase transition in LC elastomers, in which the smectic elasticity is coupled to an elastic network of cross-links that provides an *internal* random field. In this situation, the smectic layer order also disappears but—in contrast to the situation described for monomeric smectics in aerogels—only above a certain cross-link density. The smectic elastomer network appears to be quite resistant to quenched disorder. We investigate this remarkable disordering process in some detail, combining thermoelastic data and stress-strain measurements with analysis of the x-ray line shape associated with the smectic layering, which provides a detailed picture of the route to short-range layer correlations.

Liquid-crystalline order and polymer properties can be combined by attaching mesogenic molecules to a polymer backbone via flexible linkages (side-chain LC polymers). The backbone polymer—in turn—can be weakly cross-linked to form an elastomer (see Fig. 1). The macroscopic rubber elasticity introduced via such a percolating network interacts with the LC ordering field [25]. In smectic side-chain LC elastomers, the layers cannot move easily across the cross-linking points where the polymer backbone is attached. Consequently,

*Present address: DWI, RWTH Aachen University, D-52074 Aachen, Germany; dejeu@dwi.rwth-aachen.de

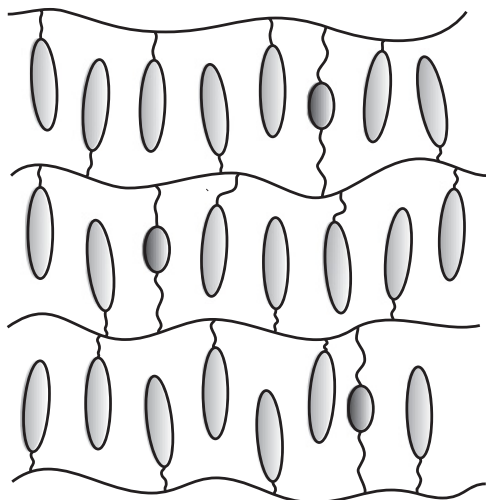


FIG. 1. Schematic representation of a smectic side-chain elastomer.

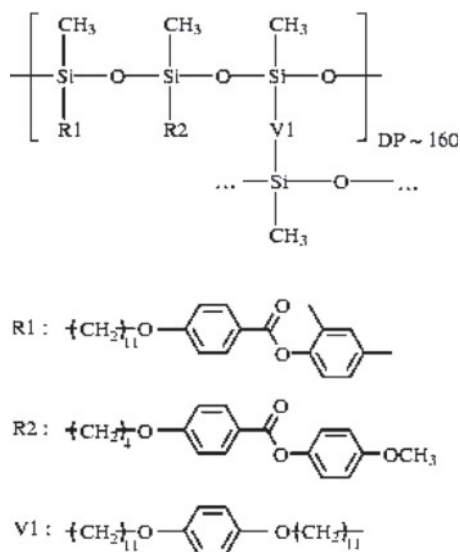
layer displacement fluctuations are suppressed, which under certain circumstances can stabilize the 1D periodic layer structure [26–28]. On the other hand, the cross-links provide a random network of defects that has been predicted to destroy the smectic order [29]. Thus in SmA elastomers, two opposing tendencies exist: suppression of layer displacement fluctuations that enhances translational order, and the effect of random disorder that leads to a highly frustrated equilibrium state. The road to layer disorder with increasing cross-link concentration has been mapped out experimentally using x-ray scattering [30,31]. The line shape shows a gradual change from a central Gaussian with power-law tails (describing finite-size smectic domains) for low cross-link concentrations, via stretched Gaussians, to a Lorentzian shape (describing extended short-range correlations) at higher cross-link densities. The present measurements relate to a similar elastomer system that displays at high temperatures additionally a transition to

a nematic phase, which modifies the approach to disorder. Above a certain cross-link density, both the smectic-nematic and the nematic-isotropic transition disappear, corresponding to a shift of the system to the parasmectic regime of a first-order smectic-isotropic transition. In the following, we present first details of the experiments and then we continue with the results and discussion.

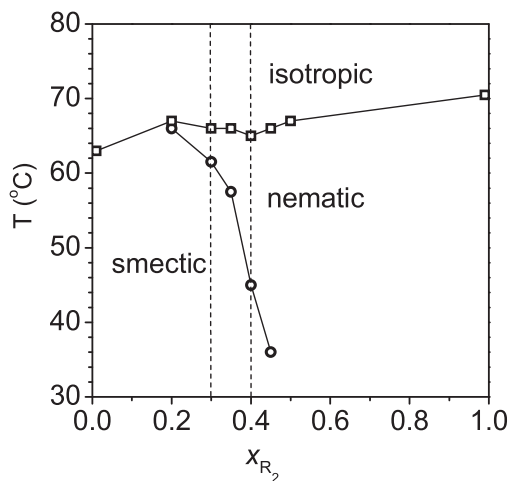
II. EXPERIMENTAL

The investigated LC co-elastomers consisted of a poly(methylsiloxane) backbone, end-on attached mesogenic sidechains R1 and R2, and a bifunctional isotropic cross-linker V1 [Fig. 2(a)]. The synthesis was carried out in a Pt-catalyzed hydrosilylation reaction of a poly(hydrogenmethylsiloxane) prepolymer and vinyl-terminated side chains in isotropic solution as described elsewhere [32]. The side chain R1 leads to a smectic-A phase, while a nematic phase is induced by addition of the group R2, as indicated in the phase diagram of Fig. 2(b). We studied the elastomer E70/30 and E60/40 with 30% and 40% of the nematogenic group R2, respectively, for two cross-link concentrations, 5% and 10%. The elastomer E70/30 has a stronger smectic tendency than E60/40, as is evident from the smaller nematic range and the twice as large layer compression modulus (see below). In this terminology, the fully smectic elastomer discussed earlier [30,31] would be indicated as E100/0. Hence the choice of these two concentrations of the nematogenic group R2 should provide a rather complete picture.

“Single-crystal” smectic elastomer samples were synthesized following a two-stage process [32,33]. In the first step, the sample is slightly cross-linked in the isotropic phase while solvent is still abundantly present. Subsequently, the solvent is removed at elevated temperature with the sample under a uniaxial load. The sample is cooled to the nematic phase in which the director is macroscopically oriented in the



(a)



(b)

FIG. 2. (a) Chemical structure of the elastomers investigated. (b) Schematic phase diagram from phase-transition temperatures of thermoelastic measurements for different nematogenic fractions R2 and 5% cross-links. The two elastomer compositions investigated correspond to the vertical lines and are designated as E70/30 and E60/40, respectively.

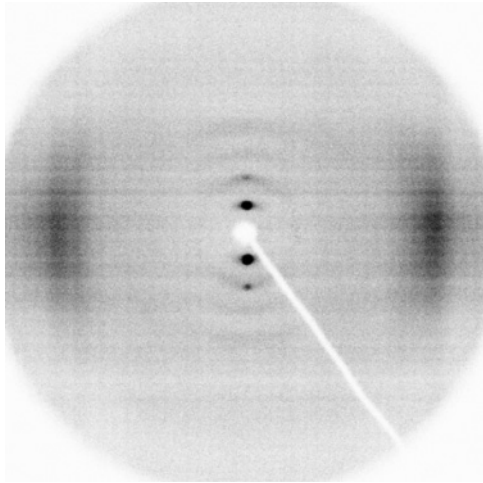


FIG. 3. X-ray overview of the smectic phase of sample E60/40 5% (room temperature).

direction of the uniaxial stress, which determines the long direction of the sample (smectic layer normal). Upon cooling to the smectic state, uniformly aligned layers build up and the orientation is fixed by a second cross-linking step in the smectic phase. To remove the soluble content, the networks were extracted several times in a mixture of isohexane and toluene. Afterward, the samples were dried in the isotropic state and cooled down to room temperature under a small load. The elastomers were still about 30 °C above the glass transition. The SmA phase was identified at room temperature through 001 and 002 quasi-Bragg peaks along the layer normal at a wave vector q_n and a broad liquidlike equatorial peak from the in-plane short-range order (see Fig. 3). Typical mosaic distributions around the smectic layer normal were around 10°

Thermoelastic measurements were carried out in a homemade oven that was kept at constant temperature for 1 h between measurements to ensure thermodynamic equilibrium. The length of the sample was measured using a digital camera. Stress-strain measurements were performed using a self-constructed apparatus. In a heated cell, the sample was stretched by two stepping motors at strain steps of about 0.5%, the stress being measured by a force-transducer. The time

between each deformation step was taken as 2 h to allow full relaxation of the sample [34].

X-ray experiments were performed at Exxon beamline X10A at the National Synchrotron Light Source, Brookhaven National Laboratory (Upton, NY) using 11.3 keV radiation (wavelength $\lambda = 0.1092$ nm). The wave-vector transfer is given by $\mathbf{q} = \mathbf{k}_f - \mathbf{k}_i$, where \mathbf{k}_f and \mathbf{k}_i are the outgoing and incoming wave vector, respectively, with $q = |\mathbf{q}| = (4\pi/\lambda) \sin \theta$, 2θ being the scattering angle. The scattering plane (z, x plane) was vertical with the q_z axis parallel to the smectic layer normal. Hence the quasi-Bragg peaks were measured in reciprocal space at q_n along q_z . Using a double-bounce Ge(111) monochromator and a double-reflection channel-cut Si(111) analyzer crystal, the wings of the resolution function were cut down to $\sim (q_z - q_n)^{-4.5}$ at small deviations from the Bragg position and to $\sim (q_z - q_n)^{-3}$ farther away. The center of the resolution function in the scattering plane was close to a Gaussian with $\Delta q_z = 0.003$ nm⁻¹ [full width at half-maximum (FWHM)]. The resolution function along the q_x direction was an order of magnitude narrower and taken as a δ function. Out of the scattering plane, the resolution was set by slits to $\Delta q_y = 0.02$ nm⁻¹. The incident intensity was about 5×10^9 cts/s; the beam size was 0.5×1 mm² ($V \times H$). All data were background subtracted, considering separately the \mathbf{q} -dependent spatial background in the hutch and the time-dependent dark current of the scintillation counter.

III. RESULTS AND DISCUSSION

Both samples with 5% cross-links show clear SmA- N and N - I transitions in their thermoelastic behavior (Fig. 4). Upon cooling from the isotropic phase, the sample length in the z direction changes abruptly upon reaching the nematic phase and increases further corresponding to the stronger orientational order. These results indicate an overall prolate chain conformation. The sample length passes a maximum, decreases slightly on approaching the nematic-smectic phase transformation, and remains constant in the smectic- A state. These results at low cross-link density are similar to those reported by Assfalg *et al.* [35] and serve as a reference for the different behavior of the samples with 10% cross-links (see below). The SmA- N transition temperature T_{NA} can be determined more precisely from an x-ray line-shape analysis,

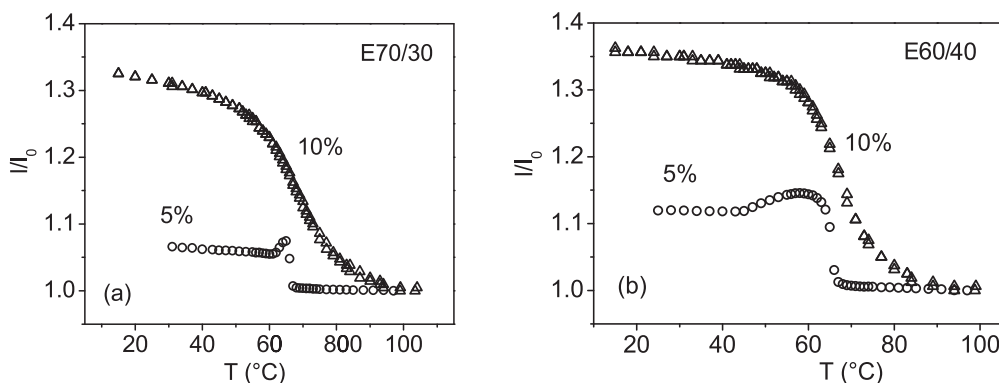


FIG. 4. Thermoelastic data for (a) sample E70/30 and (b) sample E60/40 under constant mechanical stress of 10^4 Pa.

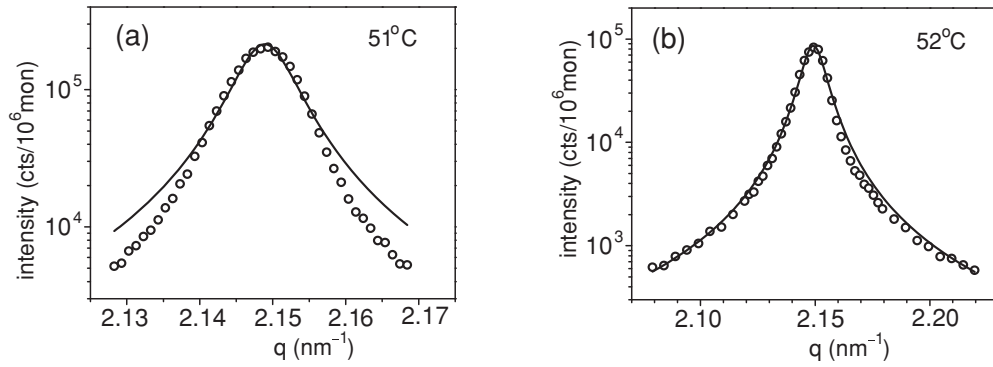


FIG. 5. X-ray line shape of sample E60/40 5% (a) just below and (b) just above the smectic-nematic transition at $T_{NA} = 52^\circ\text{C}$. The full line is a fit to a Lorentzian.

illustrated in Fig. 5 for E60/40 5%. In the nematic phase, the line shape is nicely Lorentzian, indicating short-range order characterized by a correlation length $\xi = 2/\Delta q_z$ of the order of 10–100 nm. In contrast, below T_{NA} the line shape is narrower than Lorentzian, corresponding to finite-size domains similar to those reported earlier for the purely smectic E100/0 series at low cross-link concentration [31]. From the x-ray results, no indication of the transition to the isotropic phase is found, in agreement with the paranematic nature of this transition as observed by nuclear magnetic resonance (NMR) and calorimetry of the stretched monodomain sample [36]. For E70/30, the behavior around T_{NA} is similar as for E60/40.

The stress-strain curves given in Figs. 6(a) and 6(c) show typical behavior of macroscopically oriented smectic-*A* elastomers [32,37,38]. In the direction parallel to the layer normal, a large modulus is found up to a threshold strain

$\lambda_{cr} = 1.02$. The value of E_{\parallel} of the order $(3-7) \times 10^6$ Pa corresponds to the smectic layer compressibility B . Above λ_{cr} , the modulus decreases significantly, which indicates typically enthalpic elastic behavior. On deformation perpendicular to the layer normal, a linear stress-strain relation is observed. The modulus E_{\perp} is considerably smaller ($E_{\parallel}/E_{\perp} \simeq 40$) and is close to the value obtained in the isotropic state. For E60/40, the layer compression modulus is more than twice as small as that for E70/30, reflecting the stronger nematic tendency of E60/40 [Fig. 2(b)]. Upon increasing the fraction of the nematogenic component R2 up to E50/50, a nematic phase is reached already at room temperature [Fig. 2(b)] and the ratio E_{\parallel}/E_{\perp} is reduced to 1.3, a typical nematic value [39].

For both elastomers at 5% cross-links, at room temperature second-order peaks are observed. For E60/40 5%, the peak profiles at large $q - q_n$ (Fig. 7) indicate an exponent of algebraic decay $\eta \approx 0.22$ with scaling according to $1/q^{2-n^2}$

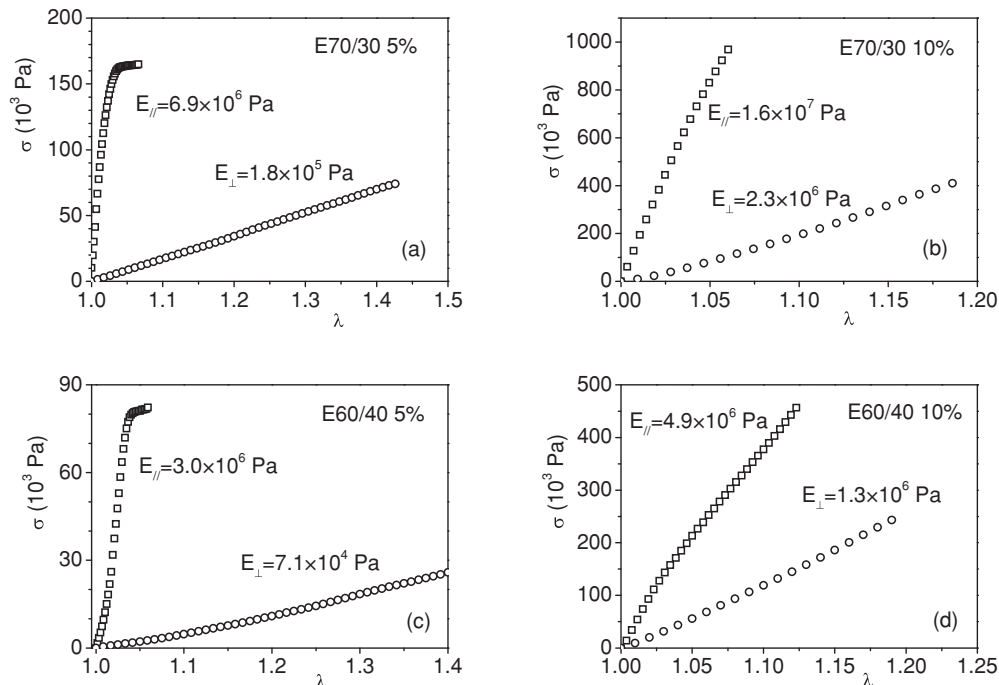


FIG. 6. Stress-strain curves for (a, b) sample E70/30 and (b, c) sample E60/40 at 25 °C. The values given for the elastic constants E_{\parallel} and E_{\perp} correspond to the initial slopes.

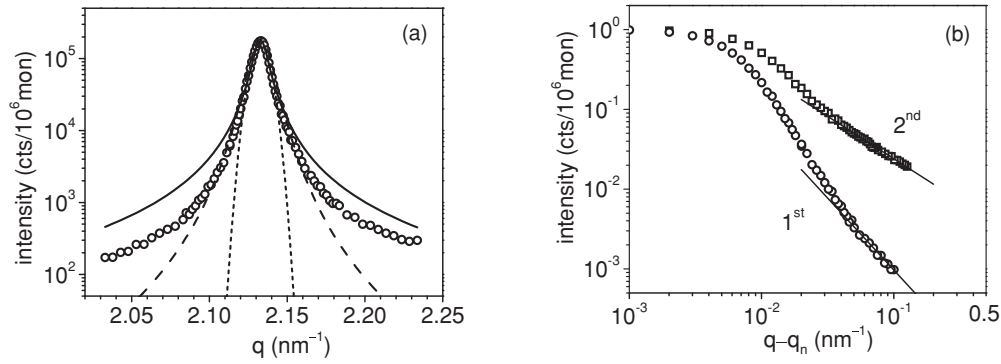


FIG. 7. (a) Line shape of sample E60/40 5% at room temperature with fits to Lorentzian (full line), square Lorentzian (dashed line), and Gaussian (dotted line). (b) Intensity profile showing power-law behavior at large $q - q_n$. Full lines have slopes $2 - \eta$ and $2 - 4\eta$, respectively, compatible with $\eta = 0.22 \pm 0.02$.

nically obeyed. Unfortunately, we could not check the temperature dependence of η as the second-order peak quickly disappears at higher temperatures. The presence of algebraic decay of the smectic order indicates that the 5% samples act disorder-free within finite domains of average size L . For E70/30 10%, also a second-order peak has been observed at room temperature. The second-order peaks are broadened by a factor of 2–3 relative to the first-order ones, indicating strain-induced broadening typical for elastomers previously stretched in the nematic phase [31]. Evidently we have not reached the limit of conventional short-range order for which

the width of successive Lorentzian peaks should vary as n^2 . In Figs. 8(a) and 8(b), the results for the 5% samples are summarized in terms of the average domain size L from the FWHM of a Gaussian fit to the line shape below T_{NA} and a correlation length ξ from a Lorentzian fit above the phase transition. The values of $L = 2\pi/\Delta q_z$ are of the order of 600–800 nm for E60/40 and about constant at 450 nm for E70/30.

The situation changes dramatically upon increasing the cross-link density to 10%. Thermoelastic measurements (Fig. 4) show neither an $N-I$ nor a $SmA-N$ phase

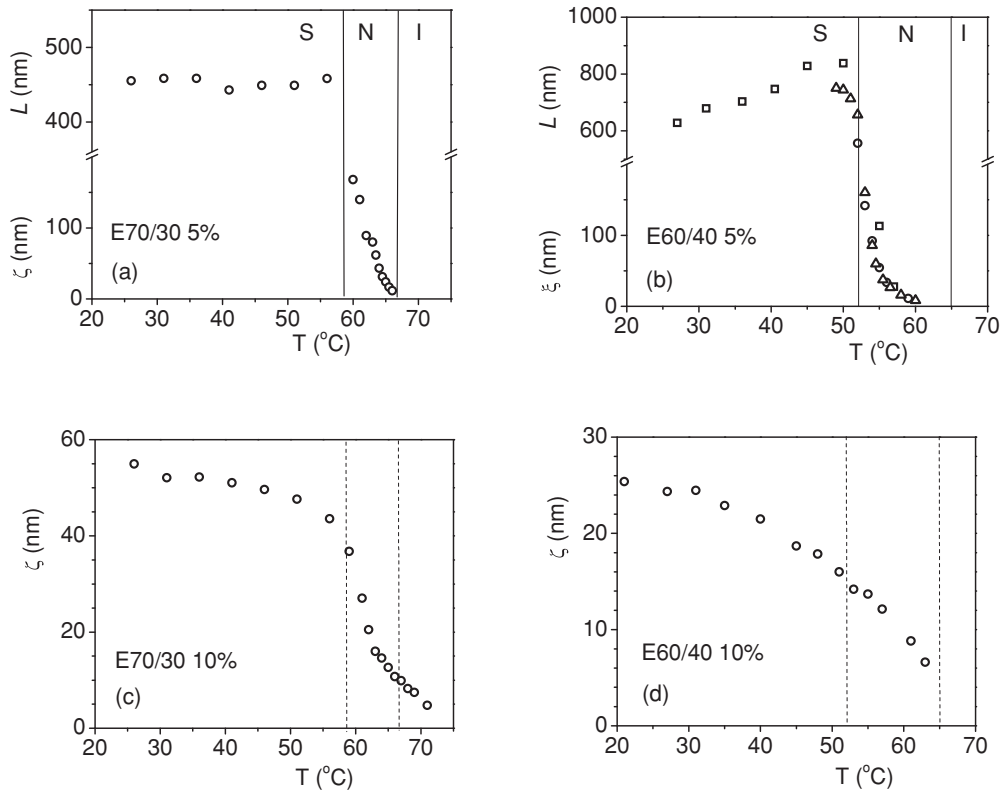


FIG. 8. Domain size L below T_{NA} (from a FWHM of Gaussian fit) and correlation length ξ above T_{NA} (from Lorentzian fit) for (a) sample E70/30 5% and (b) sample E60/40 5%. Correlation length ξ over the full temperature range for (c) sample E70/30 10% and (d) sample E60/40 10%. In (b) different symbols correspond to different runs.

transformation anymore, but a monotonic elongation of the sample in the z direction over a wide temperature range. The maximum elongation increases significantly, corresponding to a more prolate chain conformation. A similar thermoelastic behavior has been reported for nematic elastomers, which exhibit a change from subcritical to supercritical behavior with increasing cross-link concentration, as shown by 2H-NMR and high-resolution ac calorimetry [36,40,41]. Corresponding investigations of smectic elastomers have not been performed so far. In the stress-strain curves [Figs. 6(b) and 6(d)], no threshold is reached anymore in the direction along the layer normal, pointing to decreased order of the layers. The values of E_{\parallel} are nearly the same for 5% and 10% cross-links. However, the anisotropy of the moduli is now smaller: $E_{\parallel}/E_{\perp} \simeq 4 - 8$ for material with 10% cross-links to be compared with a value of about 40 for 5% cross-links. This anisotropy is known to be small in nematic elastomers, $E_{\parallel}/E_{\perp} \simeq 1$, in which resistance to stretching in all directions is due to the elastic network only. Hence the observed decrease E_{\parallel}/E_{\perp} for 10% cross-links corresponds to an approach to a more nematiclike thermoelastic response. Rather surprisingly, the decreasing anisotropy is partly due to an increase in E_{\perp} with an order of magnitude. This indicates that smectic layering persists at a small local scale and the system gets orientationally disordered. In agreement with these observations, in a wide temperature range around the former T_{NA} , all line shapes can be well described by a simple Lorentzian like in Fig. 5(b), corresponding to a disordered state. For E70/30, ξ increases continuously with decreasing temperature from 5 nm to about 50 nm, where it saturates [Fig. 8(c)]. The latter value corresponds to correlations over about 18 smectic layers. For E60/40 10%, the results are even more pronounced [Fig. 8(d)], with ξ down to only 25 nm at room temperature. For both samples, the nematic-isotropic transition is also destroyed and at long scales we have actually an isotropic phase (called paranematic, i.e., nematic at short scales but isotropic at larger ones). Experimentally, we find for the 10% samples at room temperature still some indications for algebraic decay for E70/30 but not for E60/40 anymore.

For E70/30 10%, the temperature dependence of ξ as displayed in Fig. 8(c) shows an inflection point at 61 °C. At this point, we observed a subtle asymmetry in the x-ray profile, which is related to a small shift of the maximum of the mosaic spread in the sample. Such a feature is usual for a conventional SmA- N transition for which, in correlated areas within the nematic phase, the maximum of the mosaic spread of the smectic layer normal does not necessarily coincide with the direction of \mathbf{n} . We assume that E70/30 10% below the singular point forms a randomly disordered smecticlike state with some memory of the layer normal distribution (mosaic memory), which transforms to a nematic state with thermal layer fluctuations, in which only imprinted directional memory remains. The more nematogenic compound E60/40 with 10% cross-links [Fig. 8(d)] $\xi(T)$ does not show an inflection point anymore. Moreover the saturated value of ξ at low temperatures is about twice smaller than for E70/30. The correlation length $\xi(T)$ behaves as if the sample is in a “parasmectic” regime of a first-order smectic-isotropic transition and reflects mainly changes associated with $S(T)$ and $\psi(T)$, the orientational and translational order parameter,

respectively. The positional disorder is in some sense more important as it relates more directly to layer positions than just orientations. So on short scales, it is definitely more of a dominant effect in determining the smectic correlation length. At longer scales, this positional disorder eventually peters out, i.e., randomizes the layers by no more than a layer spacing, leading to layer roughness that grows logarithmically with spatial scale. In contrast, the orientational disorder leads on long scales to unbounded growth of smectic layer roughness [42]. Note that in the purely smectic elastomer E100/0, disordering effects of similar strength occurred at a cross-link concentration of about 20% [31]. The smaller value of ξ observed in E60/40 10% can be attributed to its rather soft layer system, due to the wide nematic range and the reduced compressional modulus. Obviously, E70/30 with a larger smectogenic component represents an intermediate case between E60/40 and the purely smectic elastomer E100/0.

Interpretation of the above results is not straightforward. The results for E60/40 10% in Fig. 8(d) are reminiscent of the extended short-range layer correlations found in low-molecular-mass smectics confined in aerogels or aerosils. In both cases, the SmA- N phase transition disappears, giving way to “extended-short-range” order, in our case with a correlation length of the order of 20–50 nm. However, for elastomers this behavior occurs only at an appreciable cross-link concentration of 10%. Radzihovsky and Toner [24] studied a smectic LC in a random environment due to aerogels in the framework of the classical Landau-de Gennes model. They identified two sources of disorder: layer displacement disorder (coupling to Ψ), which represents the tendency of the aerogel to force the smectic layers to particular positions, and orientational or tilt disorder (coupling to \mathbf{n}), reflecting the inclination of the aerogel to promote particular orientations of the director (and thus of smectic layers). On short length scales, the first term is expected to be dominant, provoking disorder of the smectic state. This should occur even for arbitrarily weak quenched disorder, in agreement with experimental observations [18,20–22]. In this approach, the structure factor for x-ray scattering in a randomly disordered system can be written as

$$S(\mathbf{q}) \propto \frac{A_{\text{thermal}}}{1 + \xi_{\parallel}^2(q_z - q_0)^2 + \xi_{\perp}^2 q_{\perp}^2} + \frac{A_{\text{disorder}}}{[1 + \xi_{\parallel}^2(q_z - q_0)^2 + \xi_{\perp}^2 q_{\perp}^2]^2}. \quad (1)$$

The Lorentzian term represents the (dynamic) thermal layer fluctuations and the square Lorentzian the (static) variations in the smectic order due to the quenched random field. The correlation lengths ξ_{\parallel} and ξ_{\perp} describe the extent of local smectic order parallel and perpendicular to local nematic orientation \mathbf{n} , respectively. A similar combination of a Lorentzian and a square Lorentzian describes accurately short-range correlations induced by quenched disorder in random-field Ising magnets, and has been justified theoretically for various types of system [12,18,24]. For low-molecular-mass smectics confined to aerogels, the quasi-long-range translational order is clearly suppressed by the presence of the last term, which becomes dominant at lower temperatures. Even at very low density, the aerogels and aerosils destroy the 1D smectic

order that persists only locally on a macroscopic length scale $\xi(T) \simeq 100$ nm, the x-ray correlation length. This length is not characteristic for the aerogel structure—as would be the case for a cutoff in standard porous materials—but results from the competition between the randomizing effect of the defect network and the smectic elastic field. Thus there is no distinct SmA phase and SmA-*N* transition in such a system. The situation is different for smectic elastomers, in which algebraic decay of positional correlations survives up to a certain cross-link density. Experimentally, we find for the 10% samples at room temperature still some indications for algebraic decay for E70/30 but not for E60/40 anymore. At higher temperatures near the SmA-*N* transition, no algebraic decay comes into play anymore and the disorder term in Eq. (1) is dominant. Nevertheless, compared to aerogels, elastomer networks are more resistant to the introduction of disorder.

The source of random disorder in polymer networks is a local variation in cross-link density that manifests itself as a mechanical random field that disturbs local layer positions and orientations. The effect of cross-links on the smectic layering was introduced via a corrugated potential, which penalizes deviations of cross-links from the local layer positions [25,29],

$$F_{\text{RF}} = \gamma \int c(\mathbf{r}) |\psi(\mathbf{r})| \cos\{q_0[z - u(\mathbf{r}) + v_z(\mathbf{r})]\} d\mathbf{r}. \quad (2)$$

Here γ is the interaction strength, $c(\mathbf{r})$ is the cross-link concentration, $\psi(\mathbf{r})$ is the smectic order parameter, and $v_z(\mathbf{r})$ is the relative displacement of the rubber matrix. Equation (2) was recently evaluated further by Witkowsky and Terentjev [43] for $|\psi(\mathbf{r})| = 1$, which is valid deep in the smectic phase far below any SmA-*N* transition. Using the so-called replica trick, they integrated out the rubbery matrix fluctuations and obtained an effective free-energy density depending only on the layer displacements $u(\mathbf{r})$. For wave-vector components along the layer normal dominating over in-layer ones, $q_{\perp} \ll q_z$, and considering only long-wavelength fluctuations, the authors obtained an expression for mean-square amplitude of the displacement modes that contains a Lorentzian and a square Lorentzian term like in Eq. (1). Though different coefficients come into play, the former term again corresponds to ordinary thermal fluctuations, modified by the coupling of smectic layering to the rubbery matrix, whereas the latter term represents the effect of the random field of cross-links. Now the induced short-range order is characterized by a correlation length $\xi = (B/2\Lambda)^{1/2}$, in which the coupling constant Λ is a measure of the strength of the interaction between smectic ordering and rubbery matrix. As Λ depends linearly on the volume density of cross-links c , the relation between correlation length and cross-link density becomes

$$\xi \propto \sqrt{B/[2(c - c_{\text{min}})]}, \quad (3)$$

in which c_{min} , the minimum density of cross-links needed to form a continuous rubbery network (percolation limit [25]), has been introduced [43].

We shall attempt to make some estimates using this equation and the experimental data for ξ and B . First, at a cross-link density of 10%, the modulus B for E60/40 is a factor of 3 smaller than for E70/30. Dividing $\xi \simeq 50$ nm, characterizing the low-temperature state of E70/30, by $\sqrt{3}$, we arrive at $\xi \simeq 29$ nm, which is close to 27 nm, the value for

E60/40. Second, a reasonable value of percolation limit for the present elastomers is $c_{\text{min}} \simeq 0.04$. Then, neglecting possible differences in B , the ratio $\xi_{5\%}/\xi_{10\%}$ should be $\sqrt{6} \simeq 2.4$. Taking for E70/30 $\xi_{5\%} \simeq 150$ nm (as at the transition to the nematic phase) and $\xi_{10\%} \simeq 50$ nm at low temperatures, we arrive at a ratio $\xi_{5\%}/\xi_{10\%} = 3$ close to our estimate. However, for E60/40, the experimentally observed ratio $\xi_{5\%}/\xi_{10\%} \simeq 6$ is too large. This discrepancy could indicate that for E70/30 10%, the distortion of the layered system at low temperatures is due to random fields, whereas for E60/40 10%, the contribution from thermal disorder is still appreciable. From these observations, the following picture emerges. Smectic layer order has a more robust resistance to random cross-links than most other systems to quenched random fields. This is because in smectic elastomers, the cross-links are not rigidly frozen defects but consist of flexible chains embedded in the slowly fluctuating elastomer gel. As a result, in a pure smectic like E100/0, a rather large cross-link concentration of about 20% is needed before disorder is reached. In the present systems with a SmA-*N* transition, the increasing nematogenic tendency makes the smectic phase more susceptible to distortions, culminating in the fully disordered phase for E60/40 10%.

When interpreting the experimental results, it is important to consider how the smectic elastomer sample has been prepared. If the smectic layers are aligned by a surface or an external field and then cross-linked, we can expect the cross-links to be in registry with the smectic layers and to stabilize the lamellar structure against layer displacement fluctuations. This situation will facilitate the theoretical prediction [26,27] that, under certain circumstances, translational order can be enhanced and even become truly long-range. If the cross-linking is first done in the nematic or isotropic phase, uniaxial alignment will be accomplished in a monodomain nematic elastomer, and after the sample is cooled down to the smectic phase the result will be opposite. Though the sample will preserve uniaxial alignment, the layer positions will be frustrated due to random cross-link positioning. In that case, the cross-links provide a random network of defects that destroys the smectic order. The final thermodynamic state of the sample will depend on the relative impact of cross-linking at the first stage and at the final stage where the network is fixed. In most experiments on LC elastomers—including our present ones—“single-crystal” elastomers have been made via the two-step cross-linking process, which involves stretching in the LC state. There is increasing evidence that this situation represents a special thermodynamic state [44]. Evidently, there is room for experiments on nematic and smectic elastomer samples oriented in different ways, for example also by photo-cross-linking. In such a way, any memory of the aligning procedure imprinted in the samples may be avoided (at least partially), and probably new features of phases and phase transitions could be revealed.

In conclusion, we have put together thermoelastic data, stress-strain measurements, and high-resolution x-ray scattering data to investigate the effects of disorder due to random cross-linking on the SmA-*N* transition in LC elastomers. At a cross-link density of 5%, the algebraic decay of positional correlations in the smectic phase survives, providing a well-defined phase transition. At an increased cross-link

concentration of 10%, the smectic order disappears and is replaced by extended short-range layer correlations of the order 20–50 nm. According to thermoelastic variations, stress-strain relations, and the temperature dependence of positional correlations, both the smectic-nematic and the nematic-isotropic transitions disappear. As this only happens at an appreciable cross-link concentration, smectic layer order has a more robust resistance to a quenched random field than most other systems. For the most nematogenic compound E60/40 10%, the temperature variation of the correlation length resembles a parasmectic regime connected to a (virtual) first-order smectic-isotropic transition. The precise interpretation of these

results constitutes a major theoretical challenge for further research.

ACKNOWLEDGMENTS

We thank Leo Radzihovsky, Tom Lubensky, and Noel Clark for helpful discussions, and Steve Bennett (NSLS, Brookhaven National Laboratory, Upton) for assistance at beamline X10A. B.I.O. acknowledges partial support from the Russian Fund for Basic Research under Grant No. N09-08-00362. The Freiburg Group acknowledges financial support by the Fonds der Chemischen Industrie.

-
- [1] P. M. Chaikin and T. C. Lubensky, *Principles of Condensed Matter Physics* (Cambridge University Press, Cambridge, 1995).
- [2] L. D. Landau, *Phys. Z. Sowjetunion* **11**, 545 (1937).
- [3] R. E. Peierls, *Helv. Phys. Acta* **7**(Suppl. II), 81 (1934).
- [4] A. Caille, *C. R. Acad. Sci. Ser. B* **274**, 891 (1972).
- [5] J. Als-Nielsen, J. D. Litster, R. J. Birgeneau, M. Kaplan, C. R. Safinya, A. Lindegaard-Andersen, and S. Mathiesen, *Phys. Rev. B* **22**, 312 (1980).
- [6] C. R. Safinya, D. Roux, G. S. Smith, S. K. Sinha, P. Dimon, N. A. Clark, and A. M. Belloq, *Phys. Rev. Lett.* **57**, 2718 (1986).
- [7] D. Roux and C. R. Safinya, *J. Phys. (Paris)* **49**, 307 (1988).
- [8] D. C. Wack and W. W. Webb, *Phys. Rev. A* **40**, 1627 (1989).
- [9] E. Nachaliel, E. N. Keller, D. Davidov, and C. Boeffel, *Phys. Rev. A* **43**, 2897 (1991).
- [10] P. Štěpánek, F. Nallet, O. Diat, K. Almdal, and P. Panine, *Macromolecules* **35**, 7287 (2002).
- [11] G. Blatter, M. V. Feigelman, V. B. Geshkenbein, and A. I. L. V. M. Vinokur, *Rev. Mod. Phys.* **66**, 1125 (1994).
- [12] R. J. Birgeneau, *J. Magn. Magn. Mater.* **177–181**, 1 (1998).
- [13] A. I. Larkin, *Sov. Phys. JETP* **31**, 784 (1970).
- [14] A. I. Larkin and Y. N. Ovchinnikov, *J. Low Temp. Phys.* **34**, 409 (1979).
- [15] T. Giamarchi and P. LeDoussal, *Phys. Rev. B* **52**, 1242 (1995).
- [16] M. Chan, N. Mulders, and J. Reppy, *Phys. Today* **49**(8), 30 (1996).
- [17] N. A. Clark, T. Bellini, R. M. Malzbender, B. N. Thomas, A. G. Rappaport, C. D. Muzny, D. W. Schaefer, and L. Hrubesh, *Phys. Rev. Lett.* **71**, 3505 (1993).
- [18] T. Bellini, L. Radzihovsky, J. Toner, and N. A. Clark, *Science* **294**, 1074 (2001).
- [19] S. Park, R. L. Leheny, R. J. Birgeneau, J.-L. Gallani, C. W. Garland, and G. S. Iannacchione, *Phys. Rev. E* **65**, 050703(R) (2002).
- [20] R. L. Leheny, S. Park, R. J. Birgeneau, J.-L. Gallani, C. W. Garland, and G. S. Iannacchione, *Phys. Rev. E* **67**, 011708 (2003).
- [21] Z. Kutnjak, S. Kralj, G. Lahajnar, and S. Žumer, *Phys. Rev. E* **68**, 021705 (2003).
- [22] D. Liang and R. L. Leheny, *Phys. Rev. E* **75**, 031705 (2007).
- [23] L. Radzihovsky and J. Toner, *Phys. Rev. Lett.* **79**, 4214 (1997).
- [24] L. Radzihovsky and J. Toner, *Phys. Rev. B* **60**, 206 (1999).
- [25] M. Warner and E. M. Terentjev, *Liquid Crystal Elastomers* (Clarendon, Oxford, 2003).
- [26] E. M. Terentjev, M. Warner, and T. C. Lubensky, *Europhys. Lett.* **30**, 343 (1995).
- [27] M. J. Osborne and E. M. Terentjev, *Phys. Rev. E* **62**, 5101 (2000).
- [28] G. C. L. Wong, W. H. de Jeu, H. Shao, K. S. Liang, and R. Zentel, *Nature (London)* **389**, 576 (1997).
- [29] P. D. Olmsted and E. M. Terentjev, *Phys. Rev. E* **53**, 2444 (1996).
- [30] D. M. Lambrea, B. I. Ostrovskii, H. Finkelmann, and W. H. de Jeu, *Phys. Rev. Lett.* **93**, 185702 (2004).
- [31] E. P. Obraztsov, A. S. Muresan, B. I. Ostrovskii, and W. H. de Jeu, *Phys. Rev. E* **77**, 021706 (2008).
- [32] E. Nishikawa, H. Finkelmann, and H. Brand, *Macromol. Rapid Commun.* **18**, 65 (1997).
- [33] E. Nishikawa and H. Finkelmann, *Macromol. Chem. Phys.* **198**, 2531 (1997).
- [34] A. Greve and H. Finkelmann, *Macromol. Chem. Phys.* **202**, 2926 (2001).
- [35] N. Assfalg and H. Finkelmann, *Macromol. Rapid Commun.* **202**, 794 (2001).
- [36] G. Cordoyiannis, A. Lebar, B. Zalar, S. Žumer, H. Finkelmann, and Z. Kutnjak, *Phys. Rev. Lett.* **99**, 197801 (2007).
- [37] A. Komp and H. Finkelmann, *Macromol. Rapid Commun.* **28**, 55 (2007).
- [38] P. Beyer, E. M. Terentjev, and R. Zentel, *Macromol. Rapid Commun.* **28**, 1485 (2007).
- [39] D. Kramer, Ph.D. thesis, Albert-Ludwig-Universität, Freiburg, Germany (2010).
- [40] S. Disch, C. Schmidt, and H. Finkelmann, *Macromol. Rapid Commun.* **15**, 303 (1994).
- [41] A. Lebar, Z. Kutnjak, S. Žumer, H. Finkelmann, A. Sánchez-Ferrer, and B. Zalar, *Phys. Rev. Lett.* **94**, 197801 (2005).
- [42] L. Radzihovsky (private communication).
- [43] L. T. Witkowski and E. M. Terentjev, *Phys. Rev. E* **80**, 051701 (2009).
- [44] D. Rogez, F. Brommel, H. Finkelmann, and P. Martinoty, in *Abstracts of the 23rd International Liquid Crystal Conference, Krakow, Poland* (Jagellonian University, Krakow, 2010), p. 323.